Acoustics 2008
Geelong, Victoria, Australia 24 to 26 November 2008

Acoustics and Sustainability:

How should acoustics adapt to meet future demands?

Experimental and numerical analyses of a floating slab track

Dominik Duschlbauer (1), Matthew Pettersson (1), Geoff Lucas (1) and James Nelson (2)

(1) Bassett Acoustics, part of AECOM, Sydney, NSW 2000, Australia
(2) Wilson, Ihrig & Associates, Oakland, CA 94618, USA

ABSTRACT

A vibration isolated rail trackform, or Floating Slab Track (FST) was designed using empirical, numerical and experimental techniques. This paper focuses on the correlation between modal testing and Finite Element Analysis (FEA) of the FST. The modeshapes of the FST in the frequency range of 5 Hz to 250 Hz are discussed and the effects of adding the unsprung mass of a rail vehicle are explored within the framework of the FE method. Vibration levels measured at a slab during a train pass-by are presented. Characteristics of the pass-by spectra are explained with the developed model.

INTRODUCTION

Transit Oriented Development (TOD) is a strategy for increasing the attractiveness of more sustainable public transport over private motor vehicles. This integration of residential buildings with transport corridors creates acoustic design challenges.

The Chatswood Transport Interchange project is a TOD and includes an elevated rail station and three apartment towers within an integrated building structure.

The vibration isolated trackform was a critical part of the building design because the integrated structure of the rail station and apartment towers provided no structural breaks and promoted transmission of vibration and structureborne noise from the rail line to the apartment towers.

Vibration isolated trackforms reduce transmission of vibration from the trackform to the supporting structure by inserting an elastic element between the rail and supporting medium. Vibration isolated trackforms range in performance and complexity from rubber matting underneath rail ballast to 'floating' concrete slabs supported on rubber pads or steel springs.

For the Chatswood Transport Interchange a floating slab track (FST) was required so structure-borne noise criteria during train operation are complied with in the apartment tower above. Principal dimensions and pad layouts are presented in Figure 1. The rail vibration control measures at Chatswood also include high compliance rail fasteners, a high mechanical impedance train deck and high stiffness columns, (Nelson et al, 2008).

This paper presents results from modal tests undertaken on the FST. Dominant modeshapes up to 250 Hz are discussed and associated damping and modal mass estimates are provided. A finite element (FE) model comprising of a chain of 15 slabs is presented and 'tuned' to obtain a reasonable fit with the test data. The FE model proved to be a useful tool for exploratory studies.

The FE model was used to increase the understanding of the underlying modal regimes of the FST and to study the effects of the unsprung mass on the dynamics of the FST.

Vibration measurements during train pass-bys are presented and discussed with special attention to the effects of unsprung mass.

IMPACT MEASUREMENTS

The rail head was impacted above a resilient fastener with an instrumented hammer. The drivepoint accelerance of the rail head as well as the transfer accelerance to the closest corner of the slab were determined (Figure 2). In this paper, the drivepoint is always the rail just above a resilient rail fastener (or DF fastener). The term 'transfer accelerance' relates to the accelerance from the drivepoint to the closest corner of the slab underneath the drivepoint.

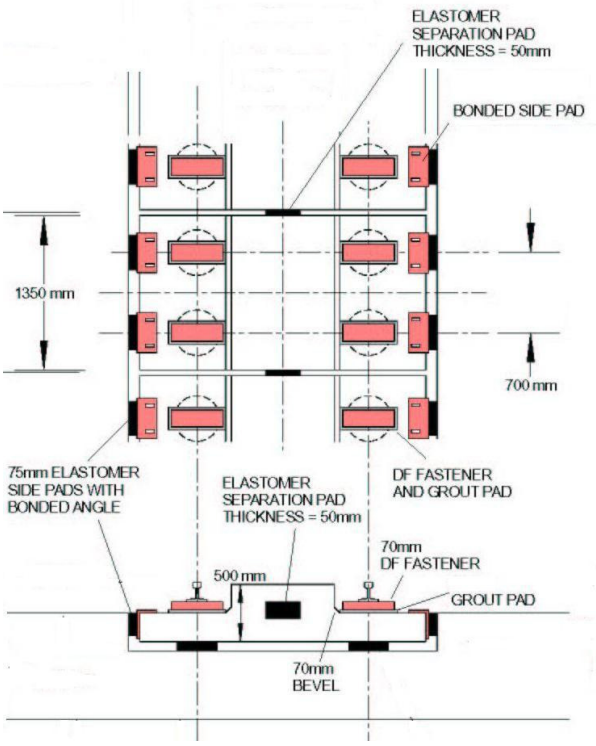

Figure 1. Schematic of the FST used at the Chatswood Transport Interchange – isolation pads are shown in black.

Three corners were instrumented allowing for determination of the rigid body modeshapes of a single slab. The sampling frequency was 2560 Hz and 4 second long timetraces per impact were recorded giving a frequency resolution of 0.25 Hz. The presented accelerance spectra were averaged over three impacts and excellent coherence was observed in the considered frequency range of 5 Hz to 250 Hz.

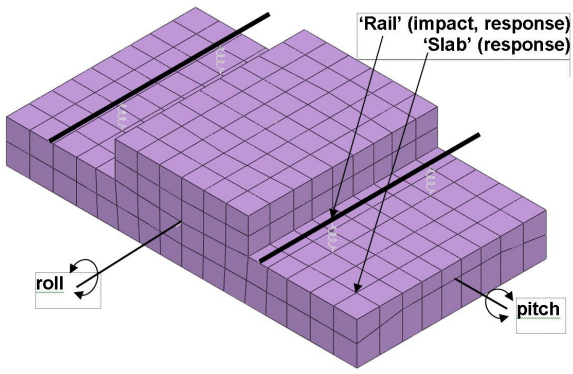

Figure 2. Impact and response location of a floating slab.

Measured accelerance spectra are presented in Figure 3. The thick black and red lines show the measured drivepoint accelerance of the railhead and the transfer accelerance to the closest corner of the slab, respectively.

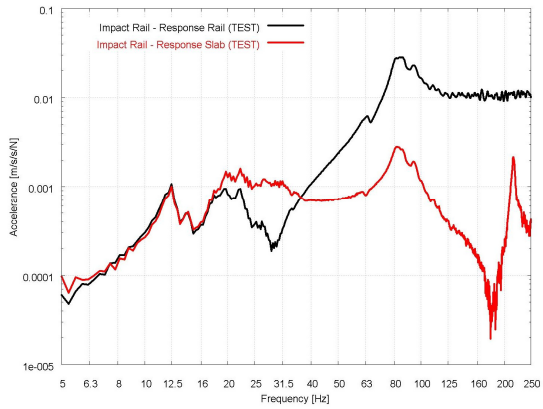

Figure 3. Measured drivepoint (black) and transfer (red) accelerance.

The fundamental mode for the FST was 12.5 Hz and the associated modeshape was found to be the slab and rail bouncing vertically with neighbouring slabs bouncing in phase. This is higher than the 11.1 Hz predicted in the initial design phase and indicates that the rubber pads are stiffer than recommended.

In the frequency range from 18 Hz to 30 Hz a high modal density is observed due to a series of rotational modes of the impacted slab and interaction with neighbouring slabs. The torsional modes in between 18 Hz to 22 Hz are rolling modes where adjacents slabs move in phase. The accelerance between rail and corner of the slab shows geometric amplification of approximately 1.5. The higher torsional modes are not as clear. As the frequency increases the global, in phase rolling of the FST becomes a rolling of individual slabs with phase lags between adjacent slabs. The motion is a superposition of roll and some pitch. For a slab's pitching motion the rail effectively acts as a stiff boundary because the bending frequency of the rail for 0.7 m nodal separation is around 1000 Hz.

The dominant mode in the drivepoint accelerance spectrum of the rail occurs between 81Hz to 85 Hz. This is the vertical rail resonance of a 60 kg rail as supported on the DF fasteners. The initial design phase predicted this mode to be at 87 Hz (Nelson et al, 2008).

The transfer accelerance to the corner of the slab shows a distinct peak at 216 Hz which is the first bending mode of the slab. This mode was predicted to be at 223 Hz in the initial design phase (Nelson et al, 2008).

The measured drivepoint accelerance was used to estimate the critical damping percentage and modal mass associated with the fundamental bending mode of the FST at 12.5 Hz and the dominant mode of the rail at 81 Hz to 85 Hz. The results are presented in Table 1.

Table 1. Estimated damping ratios and modal mass.

Frequency	12.5 Hz	81-85 Hz
% crit. damping	5.0%	6.0%
Modal mass	8600 kg	285 kg
Equivalent length	6-7 m (or ~5 slabs)	9-10 m (or ~7 slabs)

Equivalent length[1] in Table 1 gives the modal mass in terms of corresponding participating number of slabs or length of rail based on a modal mass participation factor of 0.5.

MODELLING

The Finite Element (FE) method was used to model the FST. The model was built and solved in Abaqus 6.7 (ABAQUS, 2007). The model comprises 15 slabs, which is approximately 21 metres of FST. The model size is twice the 'equivalent lengths' listed in Table 1 to ensure there is sufficient separation from boundary condition effects.

The floating slabs were modelled as rigid bodies with a total mass of 3200 kg per slab.

All elastic support pads were represented using translational springs. The platform that supports the track slab was not modelled. Instead, all springs from the slabs to the troughs and the separation pads at the each end of the chain of slabs are connected 'to ground'. The vertical stiffness of the main support pads and the side pads was 3 MN/m and 2 MN/m, respectively.

The rails were modelled using 175 mm long quadratic beam elements pinned at the ends. The DF fasteners in between rail and slab are translational springs with a vertical stiffness of 10 MN/m. The torsional stiffness of the resilient mounts was not considered.

The steady-state response of the system due to harmonic excitation at the rail head was calculated in the frequency range of interest using direct steady-state analysis. In the chosen analysis type the steady-state harmonic response is calculated directly in terms of the physical degrees of freedom of the model using the mass, stiffness, and damping matrices of the system.

Damping was modelled in terms of fraction of critical damping. From 0 Hz to 30 Hz and from 50 Hz to 250 Hz, 5% and 6 % critical damping was applied, respectively. In between 30 Hz and 50 Hz the fraction of critical damping was increased linearly from 5% to 6% critical damping.

Initially the model was solved without additional mass on the rails for correlation with the impact data. Subsequently the unsprung mass of one bogie was added and the effects on the modal characteristics of the slab were studied.

CORRELATION WITH TEST DATA

The thin lines in Figure 4 show the drivepoint accelerance (black) and transfer accelerance (red) as predicted by the FEA. In general good agreement is observed.

[1] Only the rigid body modeshapes of a single slab were determined from the impact tests. The conclusions relating to associated global modeshapes of the FST drawn in this section were confirmed with the help of a FE model (to be discussed in the next section). The FE model confirmed that the 12.5 Hz and 83 Hz modes are 'fundamental global modes' of the FST and the rail, respectively, with all sections moving in phase, similar to the fundamental bending mode of a simply supported beam. The chosen modal mass participation factor of 0.5 is that of a simply supported beam.

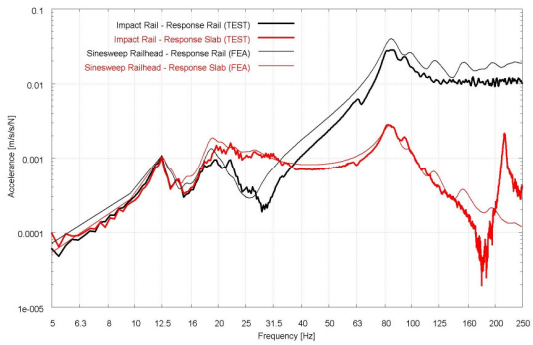

Figure 4. Measured drivepoint (black) and transfer (red) accelerance (thick black and red line) and FE based approximation (thin black and red line).

The lively rail response for frequencies greater than 100 Hz is partly attributed to the absence of torsional springs/dampers in the model. As the frequency increases, the torsional stiffness of the resilient fasteners increases to control the higher order vertical rail modes.

The measured 216 Hz slab resonance does not show in the transfer accelerance (thin red line, Figure 4) because the slabs are modelled as rigid bodies.

The deflection shapes associated with a 12.5 Hz, 19 Hz and 83 Hz sinusoidal force at the railhead are shown in Figures 5, 6 and 7. The equivalent lengths for the fundamental mode of the FST (12.5 Hz) and the vertical rail resonance (83 Hz) as listed in Table 1 are clearly identifiable.

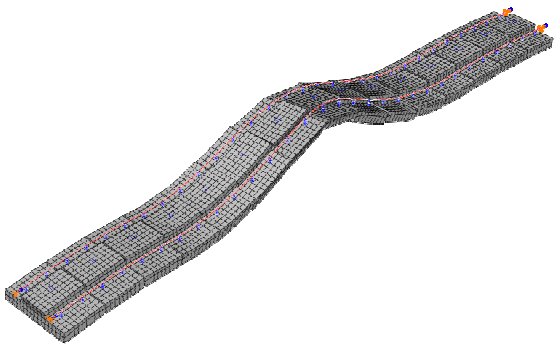

Figure 5. Deflection shape for a 12.5 Hz sinusoidal force applied at the rail head.

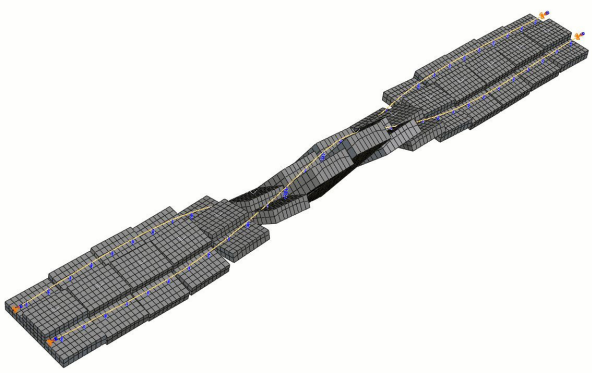

Figure 6. Deflection shape for a 19.0 Hz sinusoidal force applied at the rail head.

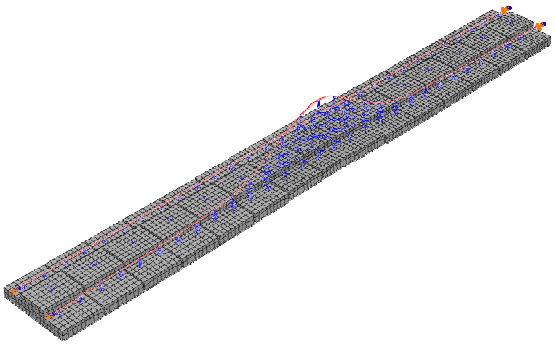

Figure 7. Deflection shape for a 83.0 Hz sinusoidal force applied at the rail head.

EFFECT OF UNSPRUNG MASS

The FE model was used to investigate the effect of the unsprung mass of a rail vehicle on the dynamic response of the FST. Two axles (320 kg/axle) and four wheels (440 kg/wheel) at 2.4 meters offset were introduced which is consistent with suburban commuter train sets in Sydney. The wheels were modelled as lumped masses attached to the ends of the axles. The translational DOFs of the rail and the axle ends were coupled. One axle was placed above the resilient rail fastener which is forced. The forcing scenario was kept unchanged and only one rail/wheel was forced for meaningful comparison.

The predicted drivepoint accelerances (black lines) and transfer accelerances (red lines) with and without the unsprung mass are compared in Figure 8.

The effect of mass shifts the fundamental mode of the FST from 12.5 Hz to 11.5 Hz. The dominant rail bending mode is shifted from 82 Hz to 36 Hz, where two wheels on each axle are moving vertically in phase. The two wheels on an axle move vertically out of phase at 42 Hz.

The accelerances of the bouncing and torsional modes at 11.5 Hz and 15Hz to 20 Hz, respectively, are hardly reduced by the presence of the unsprung mass due to the comparatively large modal mass associated with these modes.

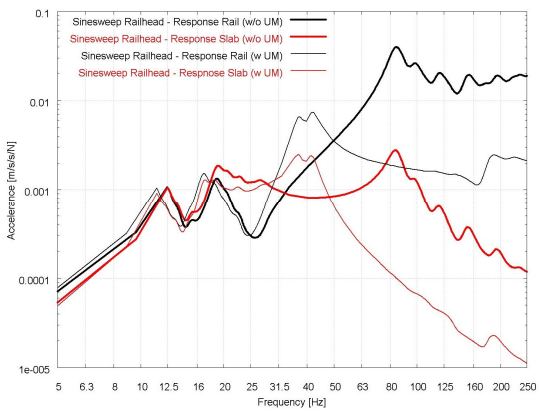

Figure 8. Predicted drivepoint and transfer accelerance (thick black and red line) without unsprung mass (thick lines) and with unsprung mass (thin lines).

The transfer accelerance from the railhead to the corner of an adjacent slab and to a corner three slabs away from the axle was extracted. The results together with the transfer accelerance of the driven slab (red line) are shown in Figure 9.

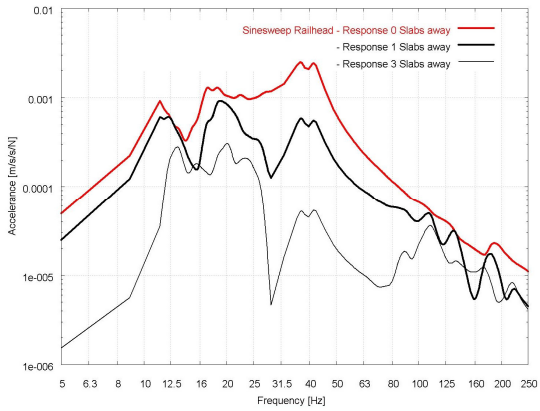

Figure 9. Effect of transfer accelerance on distance from axle.

With increasing distance from the axle the transfer accelerance decreases. The decrease has a marked dependence on the frequency and is greatest in the 30 Hz to 80 Hz range. Maximum values of the predicted transfer accelerances in the 16 Hz to 25 Hz range and the 31.5 Hz to 63 Hz range for the driven slab and 3 slabs from the driven slab are provided in Table 2. The reduction in the 31.5 Hz to 63 Hz range is more than ten times greater than in the 16 Hz to 25 Hz range.

There is minimal attenuation in the predicted transfer accelerances above 100 Hz due to a series of higher order vertical rail modes.

Table 2. Maximum transfer accelerances from Figure 9.

Frequency range	16–25 Hz	31–63 Hz
Maximum accelerance, driven slab [m/s^2/N]	1.25x10^{-3}	2.5x10^{-3}
Maximum accelerance, 3 slabs f. driven slab [m/s^2/N]	0.3x10^{-3}	0.05x10^{-3}
Reduction factor	4.2	50

TRAIN PASS-BYS

Vibration levels produced by trains travelling on the FST were measured at one corner of a slab which was located approximately in the centre of the FST. Figure 10 shows the overall acceleration levels versus time for an approaching electric multiple unit (Tangara T-set). The trainspeed was perhaps 15-25 km/h. Raised vibration levels are noticeable some 10 seconds before the actual bogie pass-by, which occurred between 37 and 38 seconds.

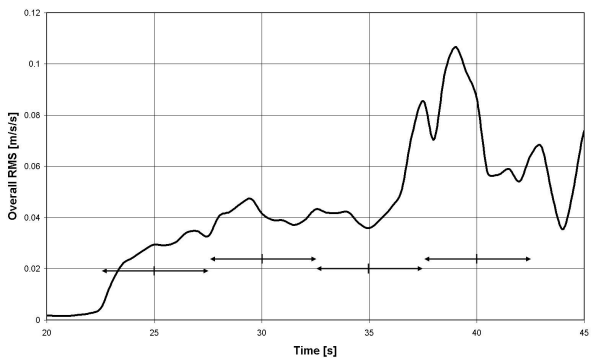

Figure 10. Overall rms acceleration measured on the corner of a slab versus time for a train pulling in.

A series of FFTs (2.5 second window length, Hanning window, 75% overlap) were calculated and converted into third octaves. The resulting spectra are shown as grey lines in Figure 11. The solid lines are averaged FFTs over the 10

second intervals marked in Figure 10. The spectra change characteristically depending on the distance of the bogie from the slab.

The forcing function used in the FEA and the actual forcing function created in the wheel/rail interface are fundamentally different. Nevertheless, by comparing relative levels in Figure 9 and Figure 11 it becomes clear that the predicted effects of unsprung mass can be observed by the slab response during actual train pass-bys.

Dominant peaks in the 40 Hz band in the pass-by spectra coincide with the axle roll-over at 37-38 seconds (Figure 10) and represent the vertical resonance of the rail and unsprung mass. In the 31.5 Hz to 63 Hz range all spectra (grey lines) 'collapse' into two regimes corresponding to a scenario with and a scenario without unsprung mass. The transition between the two regimes is almost immediate which indicates a localised effect of the rolling axle. Contrary, in the 12.5 Hz to 25 Hz range a smoother increase in vibration levels is observed as the axle approaches.

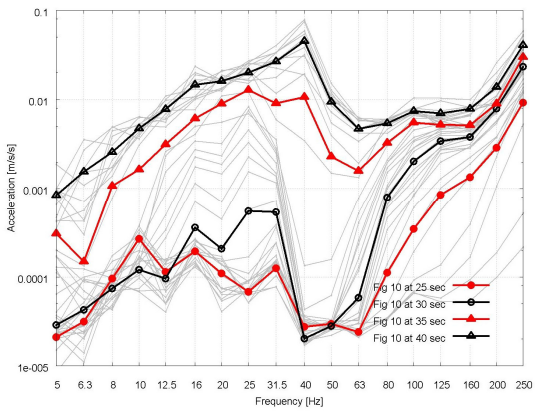

Figure 11. Acceleration spectra as measured on the slab (grey lines 2.5 second windows, 0.75 overlap).

This characteristic behaviour is also reflected in Figure 9, with the FE model predicting much greater attenuation in the 31.5 Hz to 63 Hz range than the 12.5 Hz to 25 Hz range (see Table 2).

The train pass-by spectra show that above 100 Hz attenuation versus distance is greatly reduced, confirming the predictions presented in Figure 9.

The elevated vibration levels on the slab above 200 Hz are due to the fundamental (216 Hz) and higher order slab resonances. However, elevated wheel/rail contact forces at these frequencies may also be a contributing factor.

CONCLUSIONS

Modal testing was undertaken on a FST. Damping and associated modal mass of dominant modes were extracted from the data.

A FE model was developed and tuned via the drivepoint acclerance of the railhead and the transfer accelerance to the slab. The FE model was used to visualize modeshapes and to study the effect of the unsprung wheel set mass on the rail. The later was found to be a significant factor in the frequency response functions, in particular between 30 Hz and 80 Hz.

Vibration measurements on a slab for a train pass-by were presented and the effects of the unsprung mass of the rail vehicle were discussed.

A desired future outcome of the presented FE model is to back calculate the forces created in the wheel/rail contact zone based on vibration measurements during train pass-by. This will require a different modelling approach using PSD analysis and forcing at individual wheels. Also, the effect of the sprung mass and its interaction with the slab at low frequencies and the effects on the wheel/rail contact force are of particular interest.

REFERENCES

Nelson J. T., Harrison M., Pettersson M. 2008, *Structure-Borne Noise and Vibration Control for Chatswood Interchange*, Noise and Vibration Mitigation, NNFM 99, pp. 143-149.

ABAQUS, Version 6.7, Dassault Systèmes, 2007.